Flame Retardancy and Char Microstructure of Nylon-6/Layered Silicate Nanocomposites

Kadhiravan Shanmuganathan,[1] Sarang Deodhar,[1] Nicholas Dembsey,[2] Qinguo Fan,[1] Paul D. Calvert,[1] Steven B. Warner,[1] Prabir K. Patra[1]

[1]*Department of Materials and Textiles, University of Massachusetts Dartmouth, North Dartmouth, Massachusetts 02747*
[2]*Department of Fire Protection Engineering, Worcester Polytechnic Institute, Worcester, Massachusetts 01609–2280*

Received 28 February 2006; accepted 13 August 2006
DOI 10.1002/app.25542
Published online in Wiley InterScience (www.interscience.wiley.com).

ABSTRACT: We investigated the effect of organically modified clay alone and in combination with zinc borate on the thermal/flammability behavior of nylon-6 nanocomposites. Differential thermogravimetric analysis indicated that the peak decomposition temperature was not affected by the addition of clay, but the rate of weight loss decreased with increase in clay concentration. Nanocomposite films of approximately 0.5 mm thickness with 2.5 and 5 wt % clay burned for almost the same duration as neat nylon-6 but with reduced dripping in horizontal flame test. The 10 wt % clay nanocomposite sample burned without any dripping and the flame spread rate was reduced by 25–30%. Zinc borate/clay containing nanocomposite developed into a very good intumescent system in cone calorimeter test, swelling about 10–13 mm height prior to ignition forming a cellular char structure. This was found to be an effective composition in reducing the heat release and mass loss rate of nylon-6 by about 65% and at par with 10 wt % clay nanocomposite. Flame retardant behavior could be attributed to distinct char morphologies observed through scanning electron microscopy. Fourier transform infrared spectroscopy of the 10 wt % clay nanocomposite char showed the presence of amides, indicating possible residual polymer within the shielded char. J Appl Polym Sci 104: 1540–1550, 2007

Key words: flame retardancy; zinc borate; char microstructure; heat release rate; mass loss rate; nanocomposites

INTRODUCTION

Nanocomposites are distinct class of composite materials showing impressive performance for multifunctional applications. They are defined by the particle size of the dispersed phase having at least one dimension less than 100 nm.[1] Polymer-layered silicate nanocomposites (PLSN) have been in the realm of research since 1961[2] owing to their enhanced mechanical,[3] thermal,[4] and barrier properties[5] over conventional composites with micron size fillers. The enhancement in properties is largely attributed to the aspect ratio and intercalation ability of the layered silicates, resulting in high specific surface area (Ref. 6, Chap. 4). Nanocomposites show great promise as effective fire retardants for many polymers.[7–12] Because of the upcoming restrictions on some of the current popular flame retardants, the flame retardancy of nanoparticle-filled systems or any nonhalogen alternatives need to be improved to meet the new standards. As a result, interest in this area of research has recently increased. Though significant reduction in heat release rate (HRR) of nanocomposites was reported since quite some time,[2] the flame retardancy of polymer filled with nanoparticles such as clay, carbon nanotubes, or silica has not further improved to achieve industrial acceptance.

Work done in the previous years by our group and others were focused on understanding the mechanism behind the flame retardancy of polymer-layered silicate nanocomposites. It was found that the addition of 2–5 wt % of montmorillonite reduces the peak HRR by 50–60% as compared to neat nylon-6 in cone calorimeter studies on slabs of 4–5 mm thickness. The reduction in HRR and mass loss rate was attributed to the formation of a surface char, which acted as a thermal insulation and mass barrier.[9,13] The heat of combustion, CO_2 and CO yields were not changed significantly, which indicated the predominant role of layered silicates in the condensed phase rather than in the gas phase. Since the flame retardant effects of layered silicates are more physical than chemical, the sample geometry would strongly influence the burning behavior of nanocomposite films. The nanocomposite films of thickness less than 1 mm or a fabric of nanocomposite fibers would behave much different when subjected to a flame. As the sample becomes thinner, the concentration of layered silicates would

Correspondence to: P. K. Patra (ppatra@umassd.edu).
Contract grant sponsor: National Textile Center, US Department of Commerce; contract grant number: 02-0740.

Journal of Applied Polymer Science, Vol. 104, 1540–1550 (2007)

become critical in providing a significant effect. In that case, we need to increase the concentration of layered silicates to a level sufficient to form a network of platelets and hence a strong mass barrier or alternatively the flame retardant effect of layered silicates has to be augmented by another flame retardant additive. We studied the effect of clay concentration on the flame retardant behavior of nanocomposites in relation to polymer-layered silicate interactions and char morphology. We also investigated the effect of zinc borate in enhancing the flame retardancy of PLSN.

We chose zinc borate to reinforce the flame retardant effect of layered silicates through the formation of a stable char. Decomposition of zinc borate releases B_2O_3 moiety, a low melting glass that can stabilize the char. It also releases its water of hydration (about 13–15%) at 290–450°C, which can blow the char to a foamy structure (Ref. 6, Chap. 2). Thus it could significantly influence the char morphology and hence the flame retardancy of polymer-layered silicate nanocomposites. Also it is thermally stable at the processing temperature of nylon-6.

EXPERIMENTAL

Materials

Nylon-6 was supplied by Honeywell Inc. and montmorillonite (1.34 TCN), modified with methyl dihydroxyethyl hydrogenated tallow ammonium, was provided by Nanocor Inc. Hence the term layered silicate or clay used in our literature refers to organically modified montmorillonite (OMMT). The specific surface area of OMMT is around 750 m^2/g and the cation exchange capacity is 92 meq/100 g (as per manufacturer). Nylon-6 pellets were dried in a vacuum chamber at 80°C for 16 h and OMMT was dried for 4 h at 100°C prior to melt mixing. Nanocomposite hybrids with 2.5 wt % (NCH 2.5), 5 wt % (NCH 5), and 10 wt % (NCH 10) of OMMT were prepared by melt compounding, using Brabender twin blade roller mixer. Also, nanocomposite with 5 wt % OMMT and 5 wt % zinc borate (NCH OMMT/ZnB) and nylon-6 with 5 wt % ZnB alone were prepared. Melt compounding was done at 240°C for 10 min at 90 rpm. The samples were pressed into films using Carver hot press under a pressure of 10,000 psi at 240°C for 2 min. Samples for cone calorimeter were prepared to the required dimensions using aluminum template in the hot press at 240°C for 5 min.

Characterization

Morphological studies

The intercalation and dispersion of layered silicates in the nanocomposites were studied using transmission electron microscopy (JEOL, TEM, 2010F field emission) at 200 kV. Ultra thin sections of 50–70 nm were microtomed from the nanocomposites frozen with sucrose, using liquid nitrogen. A water-filled boat was attached to the diamond knife so that the ultra thin sections could be floated in water and collected on TEM grids. The contrast of the area under study began to fade after a few minutes of beam exposure and hence all the images were taken before considerable contrast loss.

Wide angle X-ray diffraction (WAXD) was performed using Scintag diffractometer, using Cu Kα radiation ($\lambda = 0.154$ nm). Samples were scanned in the 2θ range 2–60° at a scanning rate of 7.5°/min with a 0.02° step size.

Thermal analysis

The pyrolysis behavior of nanocomposites and neat samples was analyzed by thermogravimetric analyzer (TGA) using TA instruments model Q500. The samples were heated in a nitrogen atmosphere from room temperature to 600°C at a heating rate of 20°C/min. Kinetics of the decomposition process was studied by differential thermogravimetric analysis and the activation energy was determined assuming a first-order reaction for polymer pyrolysis, using the Broido equation,[14]

$$\ln\left[\ln\left(\frac{1}{x}\right)\right] = \frac{-E_a}{RT} + \text{constant} \quad (1)$$

where E_a is the activation energy for the reaction; T the absolute temperature (K); and R the gas constant (8.314 J/mol K).

$$x = \frac{W_t - W_\infty}{W_0 - W_\infty} \quad (2)$$

where W_t is the weight of the sample at any time t, W_0 and W_∞ are initial and final weight of sample respectively.

Flammability testing

The nanocomposites films of ~ 0.5 mm thickness were subjected to flame testing (FMVSS 302) using an Atlas horizontal flame spread tester. The flame height was set to about 1.5 in. and the ignition source was applied for 15 s.

Flammability testing was also done on selected samples using cone calorimeter. Nanocomposite slabs of 100 mm × 100 mm and about 3.0 ± 0.1 mm thickness were subjected to an incident heat flux of 35 kW/m^2 and the ignition and heat release characteristics were observed.

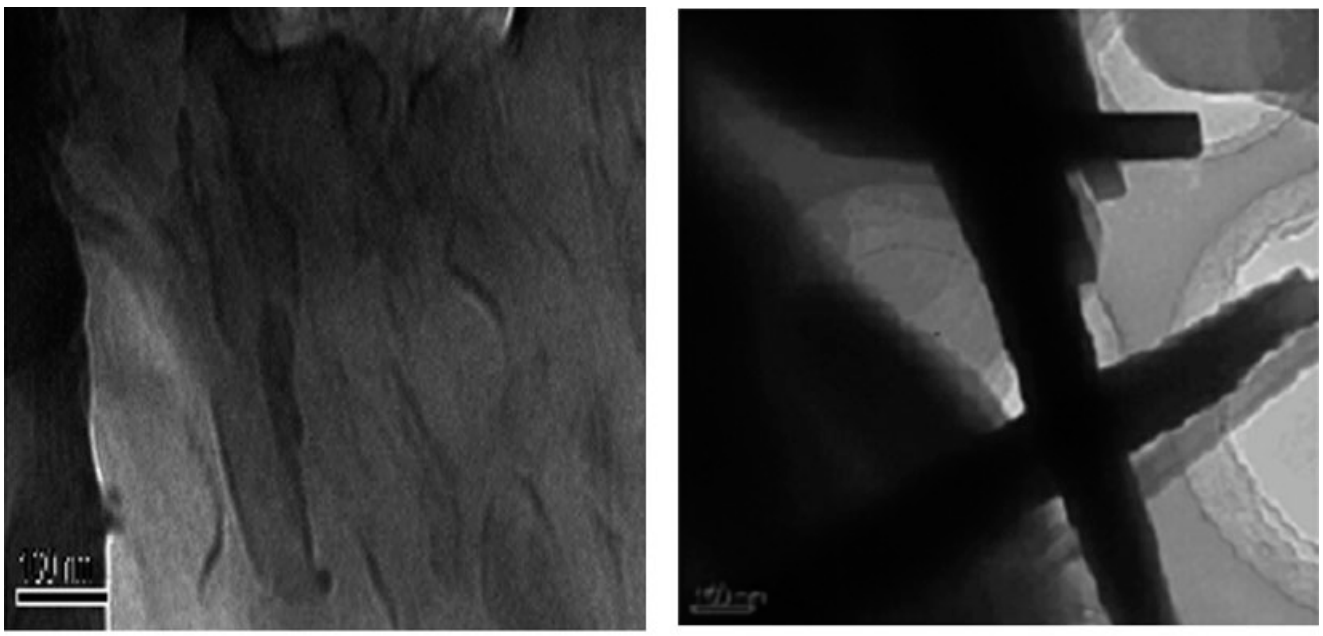

Figure 1 TEM images of (a) 5 wt % nanocomposite and (b) 10 wt % nanocomposite.

Char morphology was studied using scanning electron microscope (JEOL JSM 5610), with an accelerating voltage of 15 kV. Also Fourier transform infrared spectroscopy was done on the char using Digilab Excalibur series FTS 3000 Max in diffuse reflectance mode.

RESULTS AND DISCUSSION

Morphology and microstructure

Transmission electron microscopy (TEM) studies of the nanocomposites revealed polymer intercalation into the silicate layers (Fig. 1). With increase in concentration of fillers, the intercalation of clay is affected and agglomerated stacks are found in 10 wt % nanocomposite. WAXD patterns for the organoclay, nylon-6, NCH 2.5, NCH 5, and NCH 10 are shown in Figure 2. As seen from Figure 2(a), the organoclay shows a peak in the low angle region $2\theta = 4.54^\circ$ corresponding to a *d*-spacing of 1.944 nm between the layers. In case of nanocomposites [Fig. 2(b)], no peaks are found in the low angle (2–5°) region, which might indicate well-intercalated clay. In NCH 10 nanocomposite though a distinct peak was not observed the intensity is increasing below $2\theta = 4^\circ$, which might be due to partially intercalated structure in 10 wt % OMMT nanocomposites. This agrees with the observations from TEM images. The peaks at 10–11° and 20–24° correspond to crystal microstructure of nylon-6, which are discussed in a separate paper.

Thermal behavior

The onset decomposition temperature (5 and 10 wt % loss temperature), peak decomposition temperature, peak decomposition rate, % residue, activation energy of decomposition of nanocomposites and neat samples are given in Table I. All the temperature values are average of three readings with a standard deviation ranging from 4.04 to 5.13. The decomposition temperatures and weight loss values were affected by thermocouple performance, varying moisture levels in the samples and other factors. Though there was not a big difference in values, we observed a consistent trend in the data. It was found that the onset decomposition temperature of nanocomposites decreased as compared to neat nylon-6 [Fig. 3(a)] and the difference increased with increasing concentration of OMMT. However, the peak decomposition temperature was almost same and decomposition rate reduced with increasing concentration of OMMT [Fig. 3(b)]. The amount of additional carbonaceous residue was negligible accounting for the OMMT content.

The influence of layered silicates (OMMT) on the decomposition behavior of nanocomposites can be considered in dual aspects. The presence of enhanced polymer-layered silicate interactions favors the thermal stability of the polymer. On the other hand, the organic modifier present in the montmorillonite decomposes between 200 and 300°C and causes significant polymer matrix degradation during the melt processing of polymer organoclay mixtures.[15] It is found that OMMT and water combine to catalyze the degradation of polymer.[16] Hence, the decomposition behavior of

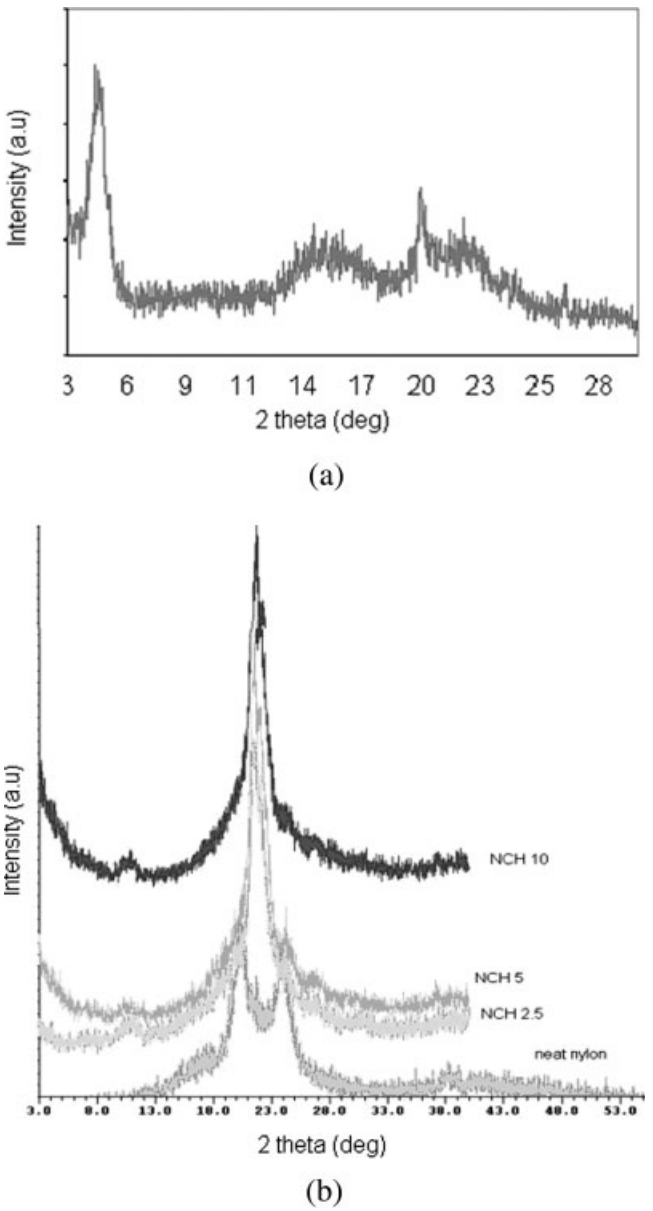

Figure 2 WAXD of (a) OMMT and (b) neat nylon-6 and nanocomposite hybrids.

nanocomposites would be influenced by the concentration of OMMT. From the values of decomposition temperature it is difficult to confirm the degradation effects of OMMT as a function of concentration. Therefore, the estimated weight loss of nanocomposites was compared with the actual weight loss as a function of temperature (Table II). The estimated weight loss was calculated using the following formula:

$$M_c = W_p M_p + W_f M_f \quad (3)$$

where M_c, M_p, and M_f are, respectively, the percentage mass of nanocomposite, nylon-6, and OMMT not yet decomposed at a particular temperature T, and W_p and W_f are the weight fractions of nylon-6 and OMMT in the nanocomposite.

It was found that up to 400°C, the observed percentage fraction of nanocomposites not yet decomposed were higher than the estimated values, based on weight fraction of polymer and OMMT. Above that temperature the observed values were less than the estimated values and the difference increased with increase in concentration of clay. This clearly showed the polymer–clay interactions and degradation effects of clay working against each other on the decomposition behavior of nylon-6. The values of activation energy for the decomposition process also decreased with increasing concentration of clay. However, the values of decomposition temperature and activation energy for 5 wt % zinc borate/5 wt % clay nanocomposite was higher than that of 10 wt % clay nanocomposite and almost close to 5 wt % clay nanocomposite, showing the dominance of degradation effect of clay at higher concentrations.

Flammability behavior

The flame-spread behavior of nylon-6/OMMT polymer films of thickness around 0.5 mm with different concentrations of OMMT (2, 5, and 10 wt %) is given in Table III. The values are average of three readings with a standard deviation of 0.27–0.76. Difficulties in visual observation of flame front and recording of time could lead to variation in measured burning time by ±3 s. Considering the limitations in measurement, it could be said that the 2.5 and 5 wt % OMMT nanocomposite films burned much the same way as neat nylon films, though the dripping tendency was reduced. However, the 10 wt % OMMT nanocomposite film burned without any dripping and the flame-spread rate was reduced by more than 40%. This assumes significant importance in practical applications. Dripping initiates

TABLE I
TGA and DTGA Data of Nylon-6 and Nanocomposites

Sample	5% wt loss temp (°C)	10% wt loss temp (°C)	Peak decomp temp (°C)	Peak decomp rate (%/min)	Residue (%)	Activation energy ($\times 10^5$ J/mol)
Neat nylon 6	432	447	488	45.59	1.009	2.24
NCH 2.5	427	444	486	45.87	2.242	2.25
NCH 5	422	440	490	37.10	5.506	1.85
NCH 10	412	436	487	39.24	8.769	1.59
NCH ZnB	420	438	484	41.36	11.03	1.82

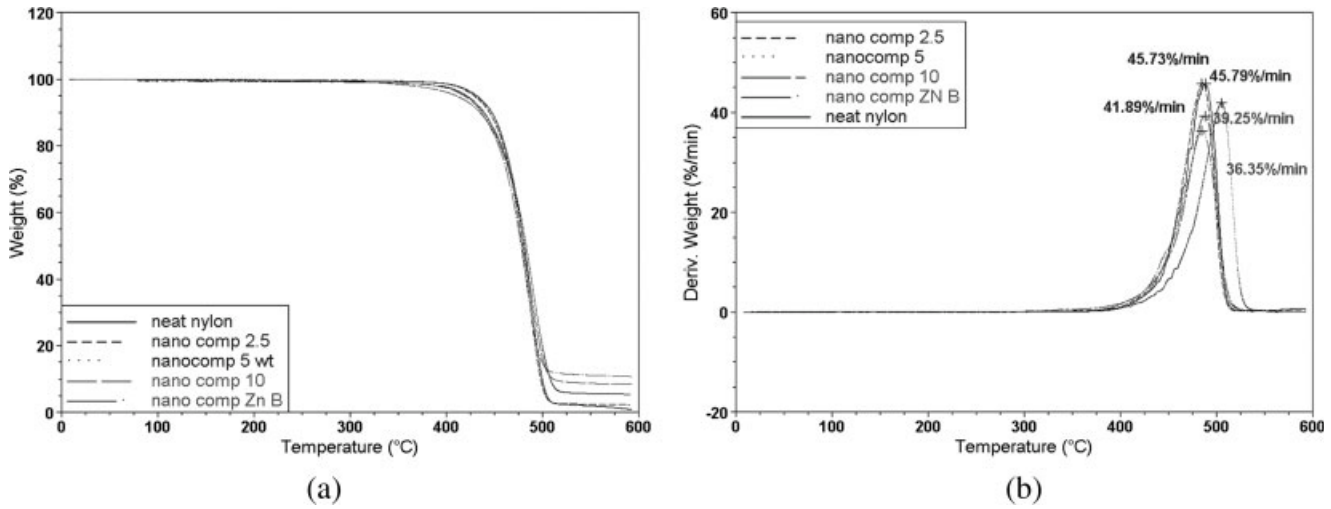

Figure 3 (a) TGA thermograms of nylon-6 and nanocomposites and (b) DTGA thermograms of nylon-6 and nanocomposites.

flame spread to surrounding materials and also increases risk of injuries during fire hazards. Reduced dripping or no dripping would be beneficial from safety point of view. The nanocomposite with 5 wt % OMMT and 5 wt % zinc borate showed very less dripping. However, the flame-spreading rate was about 50% higher than that of 10 wt % OMMT nanocomposite film (Table III).

When the concentration of OMMT is high enough to form a network structure and the material does not drip during burning, then the flame has to advance through the burnt clay. With gasification of the polymer near the flame front, the concentration of OMMT becomes high enough to form a significant mass barrier hindering the flow of volatile gases. This would significantly reduce the mass loss rate and HRR and retard flame spread. This phenomenon can be schematically represented as in Figure 4.

Morphology of char

Microstructure of char surface of the burnt nanocomposite films observed using scanning electron microscopy seems to explain well the difference in burning behavior of the nanocomposite films (Fig. 5).

The neat nylon and the NCH 2.5 film did not form an interconnected char and dripped pronouncedly during burning. The NCH 5 and NCH 10 films formed significant char on burning. However, a clear difference in char morphology could be observed between the NCH 5 and NCH 10 films. The NCH 5 film produced significant char but the char surface revealed lot of cracks and pores [Fig. 5(a)]. However, the NCH 10 film with 10 wt % OMMT formed a consolidated char [Fig. 5(b)] with very few cracks or pores. SEM image of the char cross section revealed densely accumulated clay platelets on both surfaces of char with density gradient from the center to the surface [Fig. 5(c)]. The high aspect ratio and the platelet geometry of the OMMT led to a well-interconnected network of platelets forming a protective shield. This interconnected network of platelets and viscosity effects could have restricted the dripping of the 10 wt % OMMT nanocomposite film during burning. Also, this could result in significant mass barrier effect when compared with NCH 5 film, which could explain the difference in burning rate of the films.

The addition of 5 wt % zinc borate along with 5 wt % OMMT instead of 10 wt % OMMT resulted in a significant change in char morphology [Fig. 5(d)]. The char appeared to be foamy, which might be due to

TABLE II
Weight Loss Data of Nylon-6 and Nanocomposites

	M_c					
	NCH 2.5		NCH 5		NCH 10	
Temp (°C)	Estimated	Observed	Estimated	Observed	Estimated	Observed
300	99.27	99.30	98.98	99.16	98.40	99.46
350	98.99	99.03	98.48	98.79	97.59	98.74
400	98.06	98.15	97.52	97.64	96.40	96.13
450	88.24	86.59	87.90	84.70	87.20	83.76

TABLE III
Burning Behavior of Nylon-6 and Nanocomposites

Sample	Burning behavior	Flame spreading rate (in./min)
Neat nylon	Pronounced dripping	2.04
2.5 wt % OMMT nanocomposite	Drips	1.84 (10%)
5 wt % OMMT nanocomposite	Reduced dripping	1.93 (5%)
10 wt % OMMT nanocomposite	No dripping	1.06 (48%)
5 wt % OMMT/5 wt% ZnB nanocomposite	Very less dripping	1.70 (16%)

water released during the decomposition of zinc borate. Most zinc borates in commercial use are hydrates ($xZnO \cdot yB_2O_3 \cdot nH_2O$), which release their water of hydration (about 13–15%) at 290–450°C. In addition to absorption of heat and dilution of fuel, the release of water serves to blow the char to foam.[9] The difference in char morphology could have a significant effect on the thermal insulation and barrier properties. However, cone calorimeter studies would be required to obtain more information and correlate char morphology and burning behavior.

Cone calorimeter studies

The cone calorimeter is being used extensively for flammability testing nowadays as the test reveals a lot of data useful for interpreting the combustion behavior of materials in real fires.[2] The burning behavior of nanocomposite slabs is shown in Figure 4. It is found that the burning behavior of 10 wt % OMMT nanocomposite slab differs much from the nanocomposite with 5 wt % OMMT and 5 wt % zinc borate. In the 10 wt % OMMT nanocomposite, the specimen surface started to granulate before ignition and ignition flash occurred prior to full ignition. After ignition, specimen surface burned evenly across entire surface and a well-consolidated layer of char was obtained [Fig. 6(a,b)]. However in case of nanocomposite with 5 wt % OMMT and 5 wt % zinc borate, the specimen surface started to bubble before ignition and intumesced approximately 5 mm before ignition. After ignition, specimen surface burned unevenly across surface for several seconds before burning occurred over entire surface. Also the specimen intumesced significantly to about 10–13 mm almost hitting the spark igniter. At the end a cellular char structure of about 10 mm in height was obtained as shown in Figure 6(c,d). To distinguish the role of zinc borate and OMMT on char formation process, one sample of nylon-6 with 5 wt % zinc borate was also studied. Here the specimen surface began to bubble and intumesce in a localized manner and ignition occurred unevenly for 7–10 s before flames spread over the entire specimen [Fig. 6(e,f)]. Some fragments of char were observed after burning instead of a consolidated layer. Thus it could be said that the release of water during the decomposition of zinc borate leads to bubbling and intumescence. However, it needs a char forming agent to develop the intumescence into a well-blown char structure and affect flame retardancy. The montmorillonite platelets forming a network and covering the surface serves a scaffold for forming a stable and cellular char structure along with the intumescent action of zinc borate, which could not be obtained, with zinc borate alone.

The HRR, mass loss rate, heat of combustion, smoke release, and ignition data are presented in Tables IV and V, with values in parenthesis corresponding to % change. The average values for each sample were recalculated after truncating the data corresponding to

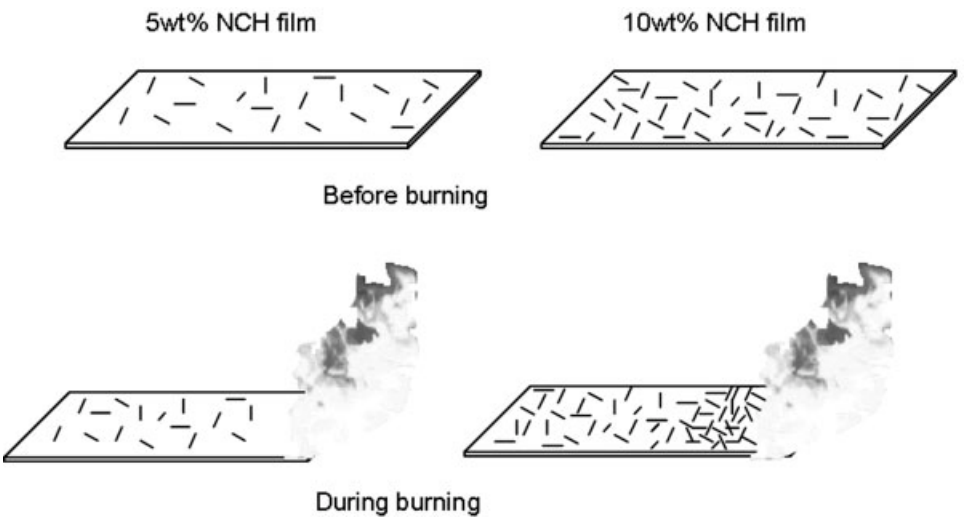

Figure 4 Schematic representation of horizontal burning behavior of films.

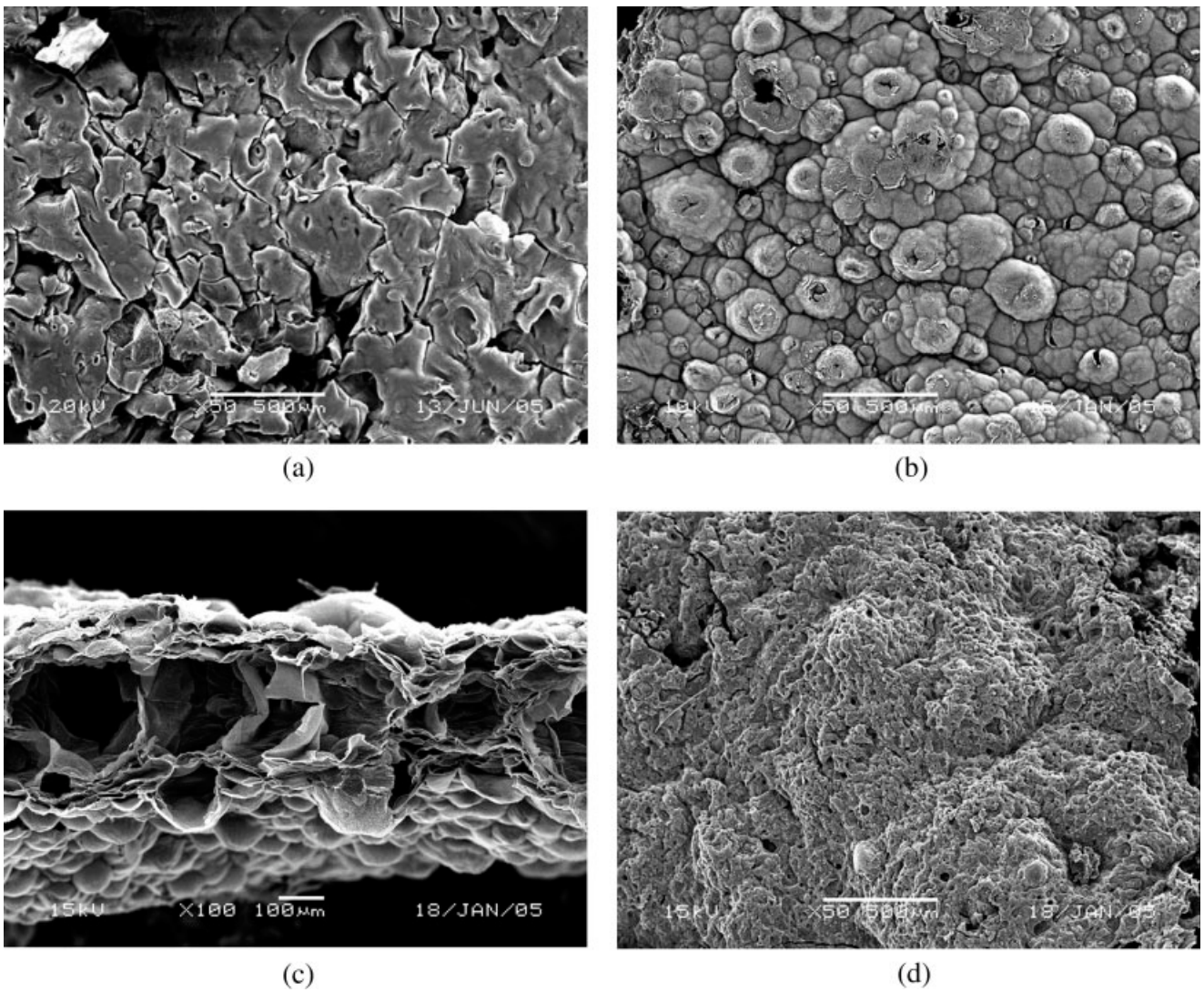

Figure 5 SEM micrograph of (a) NCH 5 char, (b) NCH 10 char, (c) NCH 10 char cross-section, and (d) NCH ZnB char.

the tail portions of the respective heat release and mass loss curves. This is to ensure that signals and noise in the beginning due to flashes and those corresponding to burning of samples in the edges are eliminated and the values represent the burning behavior of samples in the stable burning regime.

The peak HRRs of the nanocomposites were significantly lower than that of nylon-6. The addition of 10 wt % OMMT reduced the peak HRR by about 67% from 948 to 310 kW/m^2 whereas addition of 5 wt % OMMT and 5 wt % ZnB reduced the peak HRR by 69%. This is significantly higher than that of the reduction obtained with 5 wt % OMMT (54%) and 5 wt % ZnB (34%) alone. The average HRR values that are more consistent and meaningful for comparing the burning behavior of the samples also concur well with peak HRR data and revealed almost similar percentage reduction. The average mass loss rate was also reduced by more than 60% by the addition of 10 wt % OMMT or 5 wt % OMMT and 5 wt % ZnB, which mirrored the trend observed in HRR data. On the other hand, the effective heat of combustion was almost same for all samples except the 10 wt % OMMT nanocomposite sample, showing slightly lesser heat of combustion. The HRR is a product of mass loss rate and heat of combustion. With the heat of combustion remaining same it is the significant change in the rate of mass loss that has resulted in a drastic reduction in HRR.

The specific extinction area (SEA) (in m^2/g) is indicative of the smoke emission rate and given by[17]

$$\sigma = \frac{kV}{m} \tag{4}$$

where σ is the specific extinction area (m^2/g); k the extinction coefficient; V the volumetric flow rate of gases in exhaust duct (m^3/s); m the mass loss rate (g/s).

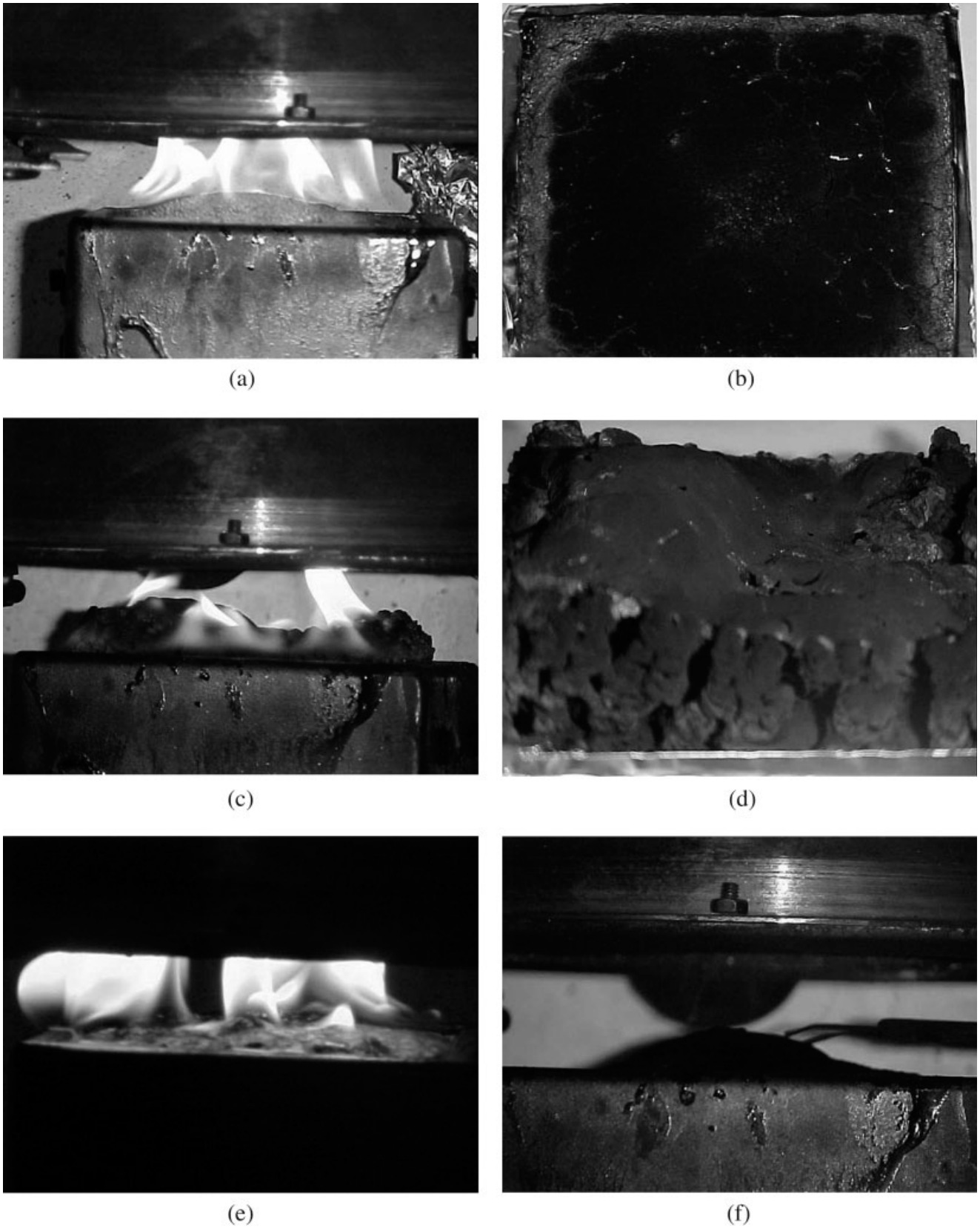

Figure 6 Digital images of burning behavior and char formation (a and b) NCH 10, (c and d) NCH ZnB, (e and f) nylon-6/5 wt % ZnB composite.

TABLE IV
Heat Release and Mass Loss Data of Nylon-6 and Nanocomposites

Sample	Peak heat release rate (kW/m^2)	Avg heat release rate (kW)	Avg mass loss rate (g/s)	Avg heat of combustion (kJ/g)	Sp. extinction area (m^2/g)
Nylon-6	948	5.04	0.18	28.04	0.099
5 wt % OMMT nanocomposite	433 (54)	2.58 (49)	0.09 (50)	28.62	0.177
10 wt % OMMT nanocomposite	310.01 (67)	1.79 (65)	0.07 (61)	25.77 (8)	0.182
5 wt % ZnB nanocomposite	624.80 (34)	2.92 (42)	0.10 (44)	27.82 (0.8)	0.184
5 wt % OMMT/5 wt % ZnB nanocomposite	289.25 (69)	1.81 (64)	0.06 (66)	27.37 (2.3)	0.196

The extinction coefficient according to de Bouguer's law is defined as

$$k = \frac{1}{L}\ln\left(\frac{I}{I_0}\right) \tag{5}$$

where L is the path length (m) across the duct, and I_0 and I are intensities of the incident light and transmitted light, respectively (W/m^2).

The specific extinction area was considerably higher for the nanocomposite samples as compared with nylon-6 (Table IV). This indicates a higher smoke emission rate of nanocomposite samples, which is in agreement with the work reported by Gilman[2] and Li and Qu[18] on EVA/MgOH/expandable graphite composites. It can be seen from Table V that the burning time of the nanocomposites is much higher than that of nylon-6. The burning time of 10 wt % OMMT nanocomposite sample was around 760 s which is more than three times that of nylon-6 (201 s), indicating slow and steady burning of nanocomposites as compared to the rapid burning of nylon-6 films. The time to ignition, however, presented a different picture with the nanocomposite samples showing much less ignition time compared with nylon-6 indicating higher volatile production in the early stages. The slight degradation of nylon-6 during melt processing in presence of additives was evident in thermogravimetric analyses. This might have caused early volatile production in nanocomposites reducing the ignition delay time.

Thus the well-consolidated protective shield like char formed by increasing the concentration of OMMT from 5 to10 wt % has been found to reduce the HRR of nylon-6 by 67% and mass loss rate by 61%. This also increased the total burning time of nylon-6 by a factor of 2–3. Addition of 5 wt % ZnB along with 5 wt % OMMT resulted in a well-intumesced cellular char of about 10–13 mm height, which also reduced the HRR/mass loss rate and other burning parameters to a similar extent as 10 wt % OMMT nanocomposite sample if not by a higher degree. However, it should be noted that while adding 5 wt % ZnB has a lower flame retardant effect as compared to 5 wt % OMMT, adding it along with 5 wt % OMMT gives similar flame retardancy as 10 wt % OMMT. This indicates the effectiveness of combining action of both additives in forming a stable protective char.

The ignition and heat release data address the flammability issue differently, with the nanocomposites showing a higher propensity to ignition but burning in a slow and controlled manner as compared to rapid burning of nylon-6. The results can be better interpreted in terms of flame-spread using an approximate model developed by Quintiere and coworkers.[19,20] They derived an analytical solution to upward or wind-aided flame spread process resulting in two dimensionless parameters a and b that could be used to indicate the potential for flame spread. The parameters are given by

$$a = K_f Q'' - 1 \tag{6}$$

$$b = a - \frac{t_{\mathrm{ig}}}{t_b} \tag{7}$$

where K_f is a constant approximately equal to 0.01 m^2/kW, Q'' is HRR value estimated from cone calorimeter (kW/m^2), t_{ig} is ignition time (s), and t_b is the time to burn out (s). The parameter a applies to burning

TABLE V
Smoke Release and Ignition Data of Nylon-6 and Nanocomposites

Sample	CO yield (g/g)	CO_2 yield (g/g)	Time to ignite (s)	Duration of flaming (s)	Flammability parameter
Nylon 6	0.006	1.783	272	201	7.53
5 wt % OMMT nanocomposite	0.005	1.730	67	390	2.73
10 wt % OMMT nanocomposite	0.000	1.93	105	760	1.65
5 wt % ZnB nanocomposite	0.000	2.57	84	391	4.40
5 wt % OMMT/5 wt % ZnB nanocomposite	0.000	1.79	83	512	1.44

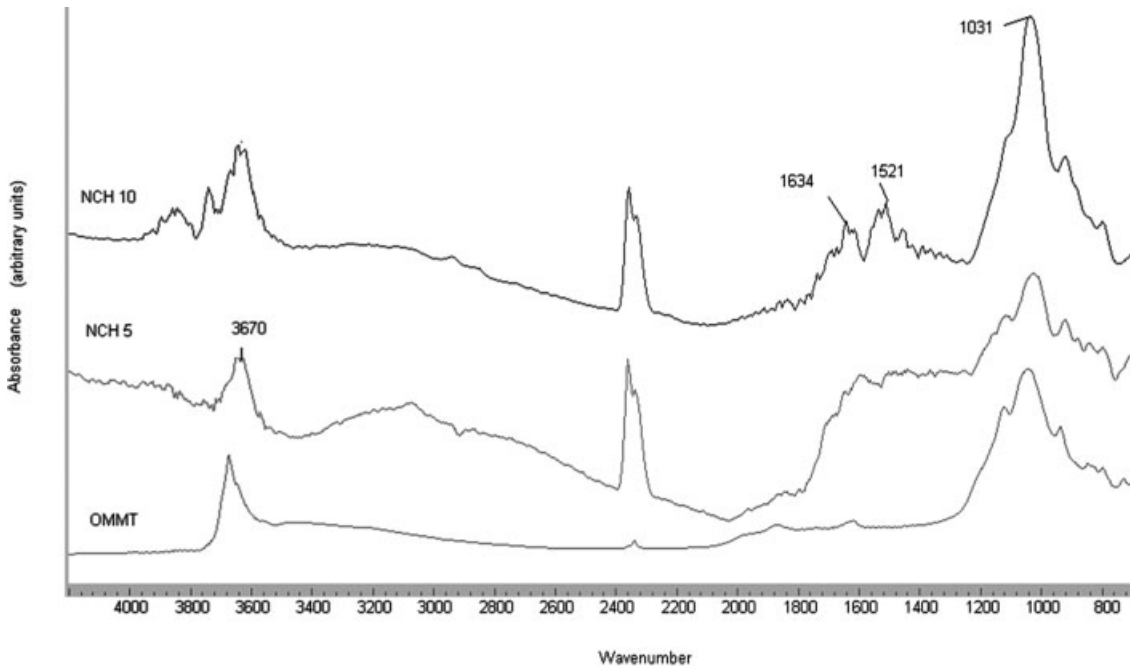

Figure 7 FTIR spectra of nanocomposite char.

materials where there is no burn out front advancing and *b* applies to materials where there is a burn out front advancing as in case of charring materials. The flame-spread process can be acceleratory, deceleratory, or steady state depending upon the value of flammability parameter. According to the model, positive value of flammability parameter indicates acceleratory flame spread and negative value indicates deceleratory flame spread while steady fire propagation can be expected when the flammability parameter is zero.

The ignition and flame spread process are sensitive to external heat flux and hence the flammability parameters and conclusions derived pertain to the specific heat flux level at which the cone calorimeter tests were conducted. We calculated the flammability parameters for the samples (Table V) using 90% of the peak HRR value as used by Cleary and Quintiere[20] and also calculated the time to burn out after truncating the data corresponding to the tail portion of HRR curves as mentioned earlier.

It can be seen from the table that the flammability parameter is positive for both neat nylon and nanocomposite samples indicating an acceleratory flame spread in all cases. However, it could be found that addition of OMMT or zinc borate along with OMMT reduces the value of flammability parameter significantly. Thus it could be said that though the addition of 10 wt % OMMT or 5 wt % OMMT and 5 wt % ZnB to nylon-6 reduced the HRR significantly and decreased the flammability parameter value from 7.5 to around 1.5, the concentration is not sufficient enough to cause a steady state or decaying flame propagation under upward or wind aided flame spread conditions.

Char analysis

The SEM image of the nanocomposite char led us to anticipate entrapment of polymer fragments between the densely accumulated clay platelets on both surfaces of char. Fourier transform infrared spectroscopy (FTIR) was conducted on clay, NCH 5, and NCH 10 char obtained from the flammability tests.

In addition to the peaks at 3670 and 1031 cm^{-1}, which represents stretching of Si—OH and Si—O, the NCH 10 char shows two additional distinct peaks at 1630 and 1520 cm^{-1}, which were not observed in clay and NCH 5 (Fig. 7). The peaks at 1630 and 1520 cm^{-1} could be assigned to amide I and amide II respectively,[21] which might indicate possible unburnt polymer fragments or recession within the shielded char. At a higher concentration, the OMMT platelets collapse to form a well-integrated shield in case of NCH 10 char as compared to NCH 5 chars (SEM micrograph, Fig. 3). This might have caused entrapment of polymer fragments and retention of unburnt chain fragments within the shielded char. These spectra are obtained from burnt char of nanocomposite film of thickness of 0.5 mm. With increase in film thickness the shielding effect of the char would be more pronounced and could result in significant retention of polymer. This would reduce the amount of fuel available for burning and might influence the burning behavior strongly.

CONCLUSIONS

Influence of clay and zinc borate on the thermal and flammability behavior of nylon-6 nanocomposite films was studied. Addition of clay was found to influence

the decomposition of nylon-6 in the early stages. However, for the concentration of clay studied (2.5–10 wt %), it could be said that the peak decomposition temperature is not affected by the addition of clay and the rate of weight loss decreases with increasing clay concentration. Horizontal flame spread tests on thin films revealed that inclusion of montmorillonite nanoparticles has a strong influence on the dripping and flame spread behavior of nylon-6 and a concentration of 10 wt % clay can completely suppress the dripping of polymer and reduce the flame spread rate by 30–40%. Inclusion of 5 wt % zinc borate along with 5 wt % MMT resulted in significant intumescence under radiant heat conditions in cone calorimeter, reducing the HRR by about 65% similar to that achieved with the addition of 10 wt % clay. This demonstrates the significance of combining the flame retardant actions of MMT and zinc borate. The char forming ability of MMT combined with the intumescent action of zinc borate is believed to have resulted in significant flame retardance. This indicates that the zinc borate/MMT combination could be a very good intumescent-based condensed phase flame retardant system for nylon-6 in the form of slabs. Thus the studies reveal that flame retardancy of polymer clay nanocomposites could be enhanced by combining the physical effect of clay with chemical action either through coating or intercalating layered silicates with flame retardant additives.

We thank Mr. Leo Barish and Mithun Shah for helping with SEM studies, Randall Harris (WPI), Frank Kozekowich, and Dave Petty (Quaker fabrics) for helping with flammability tests. We also thank Nanocor Inc. for providing the layered silicates and Honeywell Inc. for providing nylon-6.

References

1. Giannelis, E. P. Adv Mater 1996, 8, 29.
2. Gilman, J. W. Appl Clay Sci 1999, 15, 31.
3. Usuki, A.; Kojima, Y.; Kawasumi, M.; Okada, A.; Fukushima, Y.; Kurauchi, T.; Kamigaito, O. J Polym Sci Part A: Polym Chem 1993, 31, 1755.
4. Lincoln, D. M.; Vaia, R. A.; Wang, Z.; Hsiao, B. S.; Krishnamoorti, R. Polymer 2001, 42, 9975.
5. Yano, K.; Usuki, A.; Okada, A. J Polym Sci A 1997, 35, 2289.
6. Horrocks, A. R.; Price, D., Eds. In Fire Retardant Materials; Woodhead: Cambridge, 2000.
7. Zhao, C.; Qin, H.; Gong, F.; Feng, M.; Zhang, S.; Yang, M. Polym Degrad Stab 2005, 87, 183.
8. Su, S.; Jiang, D. D.; Wilkie, C. A. Polym Degrad Stab 2004, 83, 321.
9. Kashiwagi, T.; Harris, R. H., Jr.; Zhang, X.; Briber, R. M.; Cipriano, B. H.; Raghavan, S. R.; Awad, W. H.; Shields, J. R. Polymer 2004, 45, 881.
10. Morgan, A. B.; Kashiwagi, T.; Harris, R. H., Jr.; Chyall, L. J.; Gilman, J. W. Fire Mater 2002, 26, 247.
11. Song, L.; Hu, Y.; Tang, Y.; Zhang, R.; Chen, Z.; Fan, W. Polym Degrad Stab 2005, 87, 111.
12. Chuang, T. H.; Guo, W.; Cheng, K. C.; Chen, S. W.; Wang, H. T.; Yen, Y. Y. J Polym Res 2004, 11, 169.
13. Inan, G.; Patra, P. K.; Kim, Y. K.; Warner, S. B. Mater Res Soc Symp Proc 2003, 788, L8.46.
14. Broido, A. J Polym Sci Part A-2: Polym Phys 1969, 7, 1761.
15. Fornes, T. D.; Yoon, P. J.; Paul, D. R. Polymer 2003, 44, 7545.
16. Davis, R. D.; Gilman, J. W.; VanderHart, D. L. Polym Degrad Stab 2003, 79, 111.
17. Tran, H. C.; Janssens, M. L. J Fire Sci 1991, 9, 106.
18. Li, Z.; Qu, B. Polym Degrad Stab 2003, 81, 401.
19. Saito, K.; Quintiere, J. G.; Williams, F. A. In Proceedings of the First International Symposium on Fire Safety Science; Hemisphere Publishing: New York, 1986; p 75.
20. Quintiere, J. G.; Cleary, T. G. In Proceedings of the Third International Symposium on Fire Safety Science; Spon Press: Edinburgh, Scotland, 1991; p 647.
21. Chen, G.; Shen, D.; Feng, M.; Yang, M. Macromol Rapid Commun 2004, 25, 1124.